

Mathematics 4MB3/6MB3: Mathematical Biology

SPATIAL EPIDEMICS DYNAMICS: SYNCHRONIZATION

MODEL STUDENTS:

*Nicole Dumont*¹

*Melody Fong*²

*Carolina Weishaar*³

April 16, 2017

Word Count: 2175 (*so far* [http : //app.uio.no/ifi/texcount/index.html](http://app.uio.no/ifi/texcount/index.html))

¹dumontns@mcmaster.ca

²fongm5@mcmaster.ca

³weishamc@mcmaster.ca

CONTENTS

	Executive Summary	3
1	Abstract	4
2	Literature Review	4
3	Methods	4
	3.1 The Meta-patch SIR Model	4
4	Results	5
	4.1 Periods of Single Patch Model	5
	4.2 Deterministic Solution	6
	4.3 Stochastic Simulations	6
	4.4 Coherence Dependence Parameters	6
5	Discussion	6
6	Conclusion	11
	Bibilography	12

EXECUTIVE SUMMARY

In the context of disease, synchronization has been shown to inhibit rescue effects, thereby increasing the probability of eradication [1]. The objective of this study is to determine conditions in a metapopulation model that synchronize the system. The state of each patch is represented by the susceptible, infectious, and removed (*SIR*) model with sinusoidal forcing. In order to represent the effects of migration on the rate by which the disease spreads between patches, two connectivity matrices (M), equal coupling and nearest neighbour, were considered. Solutions to the model were generated using a deterministic and stochastic approach. In order to understand the behaviour of the *SIR* model for the simulated deterministic model a bifurcation diagram was generated based \mathcal{R}_0 . The solutions were generated for a 10 patch model with a 50 year life expectancy, a 13 day mean infectious period, and seasonal forcing amplitude $\alpha = 0.1$. The deterministic solutions for $m = 0.01$ became coherent if the initial conditions were close enough to the Endemic Equilibrium values. The difference between equal coupling and nearest neighbour coupling for the deterministic solution is that the nearest neighbour coupling requires more time to become coherent. In order to determine the probability of a solution becoming coherent based on different \mathcal{R}_0 and m , a 100×100 grid of \mathcal{R}_0 and m values was created. At each grid point an approximate stochastic simulation was run ten times each with different initial conditions (all within 10% of the Endemic Equilibrium values). The results of this simulation were then used in determining the probability of local extinction and the probability of global extinction. Based on the results of the study it is observed that high mixing, coherence is dips in regions corresponding to periods of less complex dynamics, especially in the period of bi-annual cycles between $15 < \mathcal{R}_0 < 25$. But, this pattern of dipping is not seen in the period of annual cycles between $\{5 < \mathcal{R}_0\} \cap \{\mathcal{R}_0 > 27\}$. Therefore, as stated in Earn, Levin, and Rohani, the results indicate that there is only a weak, if any, relation between chaos and population persistence[2] and therefore, that of the parameter \mathcal{R}_0 and coherence. In addition to this, deviations are lower for high mixing parameter and dips in the global extinction rate in comparison to the local extinction rate. This result implies that, for low coherence, the probability of global extinction and local extinction is relatively low.

1 ABSTRACT

Text goes here.

2 LITERATURE REVIEW

Long-term incidence records of many childhood diseases, such as measles, exhibit recurrent epidemics with both regular (annual, biannual and even tri-annual cycles) and irregular dynamics [2]. In countries where measles immunization is systematically distributed at 15 months and at 6 years, the observed amplitude of the incidence curve declines and the period of the epidemics become more irregular. However, overall this does not antagonize the natural dynamics of the disease [3, 2]. As a result, in order to increase the efficiency of control health care measures, it is essential to understand the factors that allow a follow up epidemic to occur after the aversion of an epidemic. In regards to childhood diseases, researchers have previously speculated that the phenomena of recurrence can be attributed to factors such as seasonal forcing, age structure models, spatial heterogeneity in terms of synchronization, and more [4]. However, many of these models have been found to be ineffective or possibly overfitted [4].

One characteristic of disease spread that has been found to accurately induce persistence within compartmental models is spatial dynamics. To induce this property, a metapopulation model is utilized, where the population is divided into several discrete subclasses called patches, each exhibiting a well-mixed population. This model is analogous to the observed population distribution within countries, where the population is concentrated throughout towns and cities. As a result, sub-populations can exhibit a variety of states, which are out of phase in contrast to the disease state observed by the entire population. For example, weekly incidence measles data from Birmingham, Newcastle, Cambridge, and Norwich recorded between 1944 and 1958 clearly show that the epidemics are in phase in Birmingham and Newcastle and out of phase in Cambridge and Norwich [5]. Asynchronous dynamics facilitate rescue effects, where the dispersal from patches with a large population prevents local extinctions in patches with small populations, thereby prolonging the eradication of disease. Hence, synchrony inhibits such processes, and could have a strong influence on the vulnerability of a disease from becoming eradicated globally. In addition to this, the facilitation of migration in modern society has allowed synchronicity to be of importance on a larger scale [1]. For example in the case of Hepatitis B, Gay and Edmunds argue that it would be more cost effective

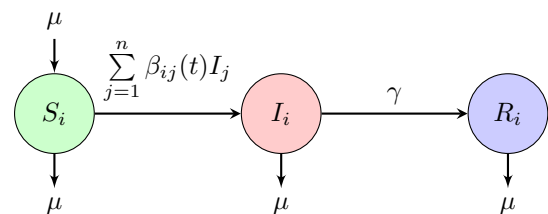
for the United Kingdom to sponsor a vaccination program in Bangladesh than a national universal program [6].

In this study, we have used a metapopulation model where the state of each patch is modelled by the susceptible, infectious, and removed (*SIR*) model. The parameters chosen are based on the expected \mathcal{R}_0 value for measles. In addition, this study makes use of sinusoidal seasonal forcing on the transmission rate in order to estimate the effects of vacation on the contact rate between the infectious and susceptible population, as opposed to the school year. The aim of this study is to analyze the dynamics of this model over time, in order to determine which parameters lead to a synchronous state, thereby eradicating the disease.

3 METHODS

3.1 The Meta-patch SIR Model

The spatial SIR model consists of n identical patches (which represent cities or some other spatial grouping of people) with identical population sizes. The population is constant in each patch and there is no migration between patches. Intra-patch dynamics are given by the standard SIR model with vital dynamics and sinusoidal seasonal forcing. Connectivity between patches is represented by disease transmission. Infected individuals can infect people from other patches. This models individuals visiting other patches, creating additional sources of infection in the visited patch. A visualization of the dynamics in a single patch i is shown by



where S_i is the proportion of the population in patch i that is susceptible to becoming infected, I_i is the proportion of the population that is infected, and R_i is the proportion of the population that has recovered and now has lifelong immunity to the disease. $\frac{1}{\mu}$ is the average life expectancy, and $\frac{1}{\gamma}$ is the mean infectious period.

The equations describing the dynamics in a single

patch are

$$\begin{aligned}\frac{dS_i}{dt} &= \mu - S_i \sum_{j=1}^n \beta_{ij}(t) I_j - \mu S_i \\ \frac{dI_i}{dt} &= S_i \sum_{j=1}^n \beta_{ij}(t) I_j - \gamma I_i - \mu I_i \\ \frac{dR_i}{dt} &= \gamma I_i - \mu R_i\end{aligned}\quad (1)$$

where S is the proportion of the population that is susceptible to infection, I is the proportion of the population that is infectious, and R is the proportion of the population that has recovered from the disease (and have lifelong immunity) or who have died as a result of the disease. μ is the birth/death rate, γ is the recovery rate, and $\beta_{ij}(t)$ are the elements of the $n \times n$ matrix $\beta(t)$:

$$\beta(t) = \langle \beta \rangle (1 + \alpha \cos(2\pi t)) M \quad (2)$$

$\langle \beta \rangle (1 + \alpha \cos(2\pi t))$ is the standard sinusoidal forced transmission rate. M is a matrix describing the connectivity between patches. Its (i, j) element is the proportion of contacts of individuals in patch i make with individuals in patch j . The off-diagonal elements are generally less than the diagonal elements since it is usually assumed individuals have more contact with people in their own patch. M is assumed here to be symmetric - i.e. patch i has as much contact with patch j as j does with i . The column sums of M (and thus the rows sums too) are all equal to one - i.e. M is doubly stochastic. This means that all of an individual's time is accounted for.

Two different types of M matrices are used in this paper. The first is equal coupling where all patches are equally connected, i.e. all off-diagonal elements of M are equal. The fraction of time individuals spend outside their own patch is given by the parameter m .

$$M = \begin{bmatrix} 1-m & \frac{m}{n-1} & \frac{m}{n-1} & \frac{m}{n-1} \\ \frac{m}{n-1} & 1-m & \frac{m}{n-1} & \frac{m}{n-1} \\ \frac{m}{n-1} & \frac{m}{n-1} & 1-m & \frac{m}{n-1} \\ \frac{m}{n-1} & \frac{m}{n-1} & \frac{m}{n-1} & 1-m \end{bmatrix}$$

The second motif is nearest neighbour coupling. In this case, it is assumed that the patches reside on a ring and

people can only visit their two nearest neighbours.

$$M = \begin{bmatrix} 1-m & \frac{m}{2} & 0 & 0 & \dots & \frac{m}{2} \\ \frac{m}{2} & 1-m & \frac{m}{2} & 0 & & \vdots \\ 0 & \frac{m}{2} & 1-m & & & \\ 0 & 0 & & \ddots & & \\ \vdots & & & & \ddots & \frac{m}{2} \\ \frac{m}{2} & & & & \dots & \frac{m}{2} & 1-m \end{bmatrix}$$

Realistic connectivity probably lies between these two extreme motifs [2].

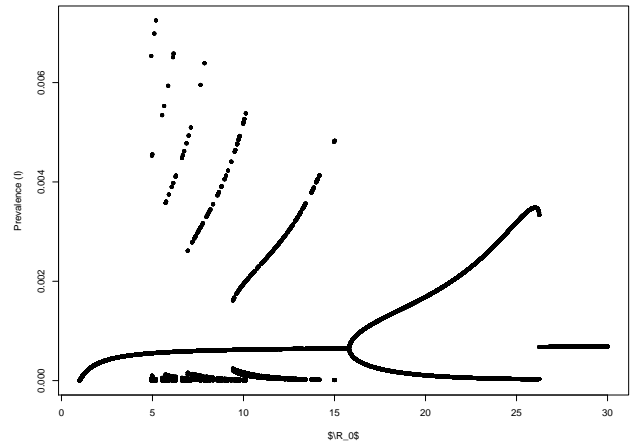
A solution to this model is said to be coherent if at all times, $I_1(t) = I_2(t) = \dots = I_n(t)$ for all n patches [1] - i.e. all states are equal to the mean $I_i(t) = \langle I(t) \rangle$. A solution is less coherent the further all states are from the mean. We use the coefficient of variation (also called the relative standard deviation) as a measure of how coherent a solution is. The coefficient of variation is the standard derivation of the set $\{I_i(t)\}_{i=1}^n$ divided by the mean of the set. If it is zero for all time, the solution is coherent.

4 RESULTS

4.1 Periods of Single Patch Model

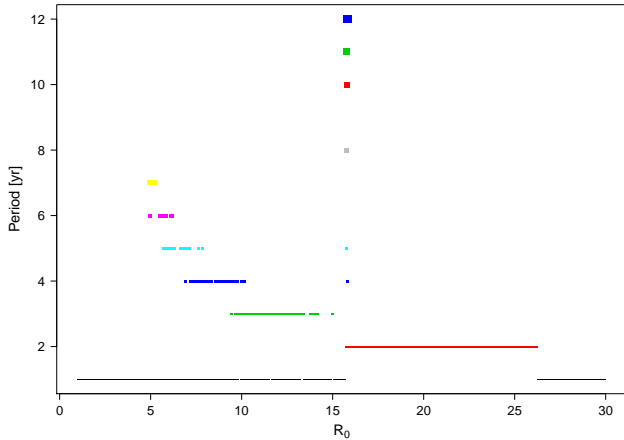
A bifurcation diagram was created using XPPAUT. This produces a bifurcation diagram which shows the periodic recurrence patterns for the simulated deterministic model of the epidemic pattern. As shown in Fig. 1, there is a single period 1 orbit for $\{5 < \mathcal{R}_0\} \cap \{\mathcal{R}_0 > 27\}$ as well as a single period 2 orbit for $15 < \mathcal{R}_0 < 25$ and mixed dynamics elsewhere.

Figure 1: A bifurcation diagram for the single patch sinusoidal forced SIR model.



Further analysis of the bifurcation diagram reveal the period compositional structure. See Figure 2.

Figure 2: The periods of the single patch sinusoidal forced SIR model vs parameter \mathcal{R}_0 .



4.2 Deterministic Solution


Solutions to (1) were calculated using the  deSolve package. The following figures are the solutions for a 10 patch model with a 50 year life expectancy, a 13 day mean infectious period, and seasonal forcing amplitude $\alpha = 0.1$. The initial conditions used were values within $\pm 30\%$ of the (S, I, R) values at the Endemic Equilibrium of the unforced single patch SIR model. In Fig. 3 values of $\mathcal{R}_0 = 17$ and $m = 0.2$ were used and the difference between equal coupling and nearest neighbour coupling is shown. It takes longer for solutions to become coherent when using nearest neighbour coupling.

Fig. 4 shows the different oscillatory periods of the epidemic cycles for two different values of \mathcal{R}_0 . In Fig. 5 weaker connectivity was used, $m = 0.01$. Solutions became coherent even at this low m if the initial conditions are close enough to the Endemic Equilibrium values.

4.3 Stochastic Simulations

A stochastic version of this model was simulated approximately using the adaptive tau-leaping algorithm. The same parameters and similar initial conditions to the ones used for the deterministic solution were used. Fig. 6 shows two stochastic simulations with $\mathcal{R}_0 = 17$ and a population of 500,000.

4.4 Coherence Dependence Parameters

The effect parameters had on coherence was investigated. A 100×100 grid of \mathcal{R}_0 and m values was created. At each grid point an approximate stochastic simulation was run ten times each with different initial conditions (all within 10% of the Endemic Equilibrium values) and the measure of coherence during the 9th year of the simulation was recorded. If the measure of coherence was below a threshold value of 0.15 (i.e. the states were within 15% of the mean value), the simulation was said to be coherent. From this, the probability of a solution becoming coherent for different \mathcal{R}_0 and m was determined. See Fig. 7.

Fig. 8 shows the probability of local extinction (the probability that the infected population of any given individual patch will go below a small threshold value), the probability of global extinction (the probability that the infected population of all patches will go below a small threshold value) in addition to the probability of coherence for different parameters.

Both of these figures are reproductions of Figs. 2 and 3 in [2] using the forced meta-patch SIR model in lieu of the logistic map function.

5 DISCUSSION

(i) First two figs < – there exist local convergence around 30% of the endemic equilibrium (where there is asymptotic stability for $\mathcal{R}_0 > 1$), so results so stick within that region [Note: maybe mention this in results somewhere (included in v2 of supplementary)] (iii) Third two figs < – relation between \mathcal{R}_0 and coherence [Note: not much info here - can remove or change to show more varied dynamics between two \mathcal{R}_0 parameters]] The most evident parameter af-

fecting the synchronization of the multipatch system is the connectivity. As shown in 6, for two models under the same connectivity relation (equal coupling), the one with higher mixing parameter m is more likely to become coherent for all time. This relationship is shown on a larger scale in Fig. 7 with the general trend of the surface sloping towards total coherence for increasing mixing parameter m . In general, this result indicates that, for example, when only changing the system by restricting the mixing of the disease by around 20%, coherence decreases from $95.2\% \pm 2.43\%$ to $77.3\% \pm 12.5\%$ [Note: Axis of coherence adapplot change from 1-0]. Therefore, in theory, increasing contact between population patches would greatly aid in synchronizing the system. However, while a synchronized system is

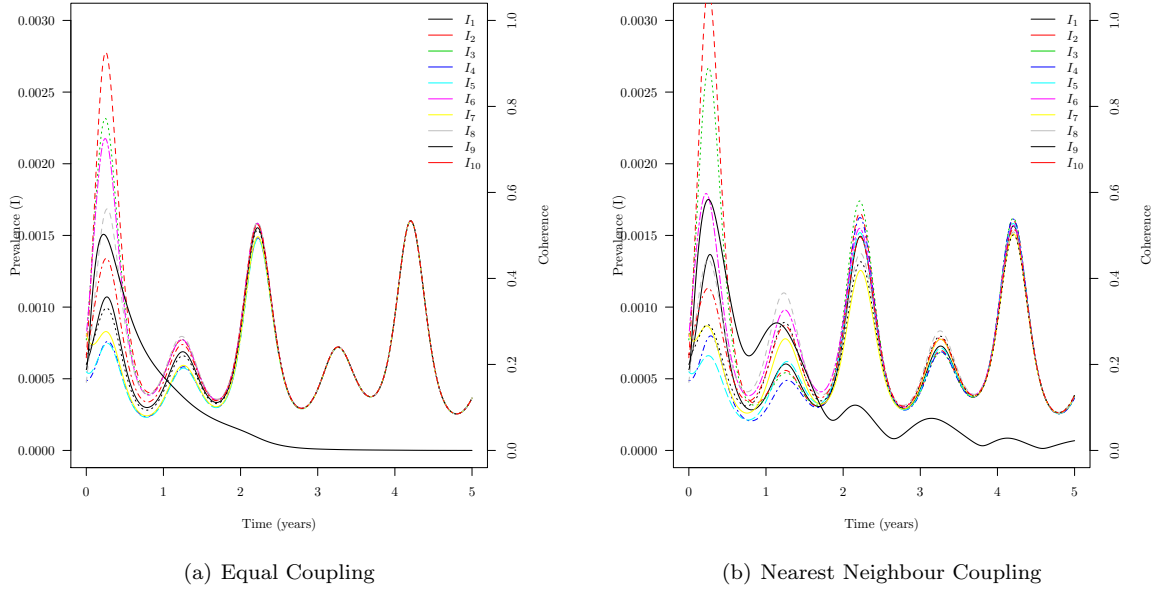
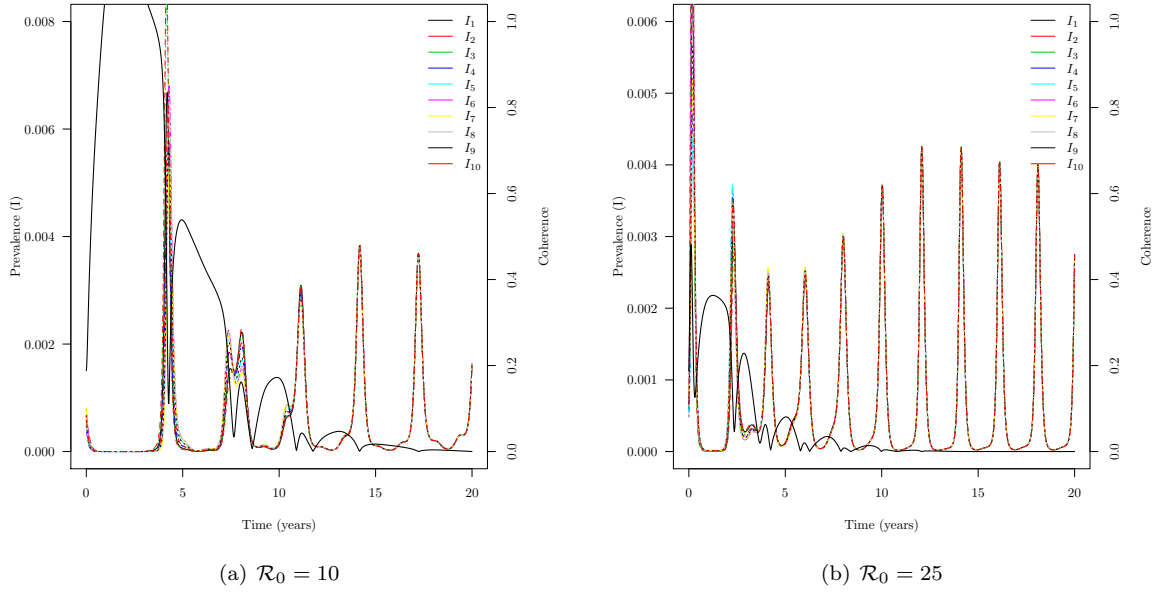
Figure 3: $\mathcal{R}_0 = 17$ and $m = 0.2$ **Figure 4:** Nearest Neighbour Coupling, $m = 0.2$ 

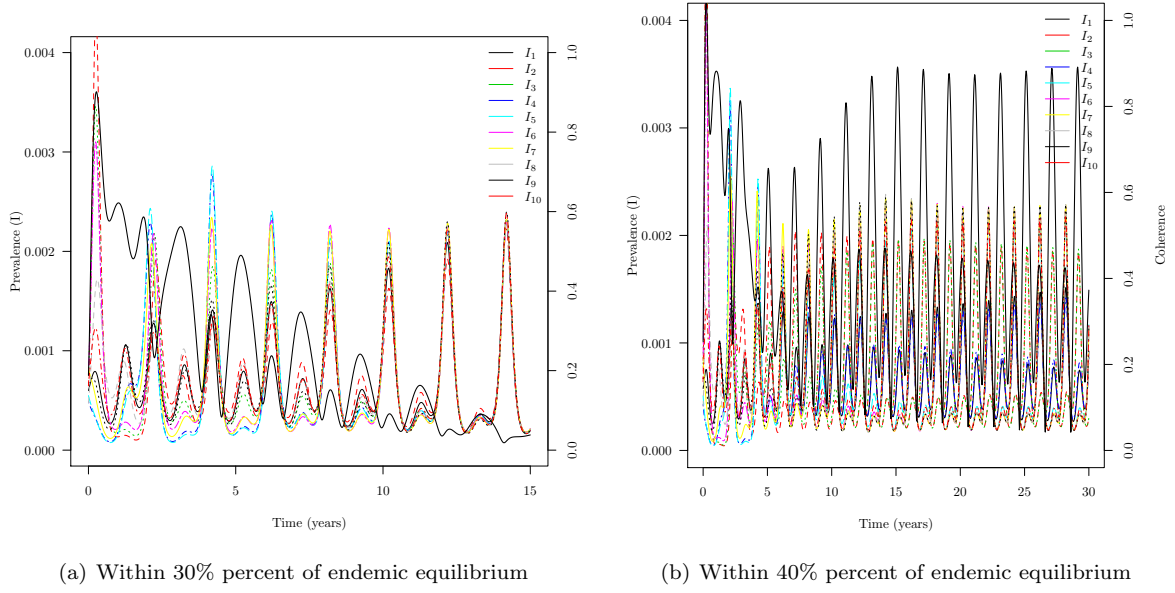
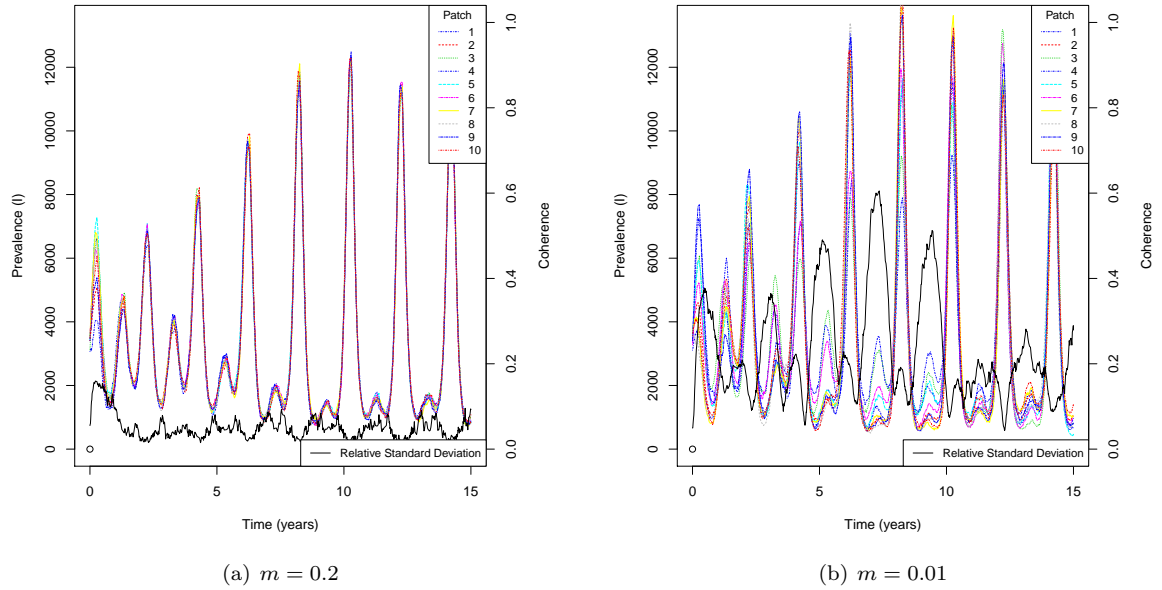
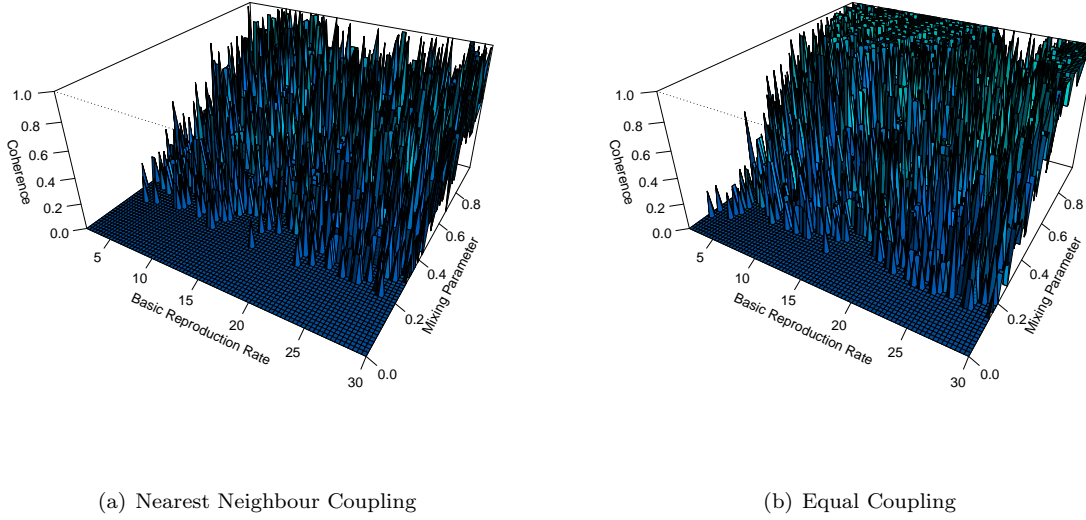
Figure 5: Nearest Neighbour Coupling, $\mathcal{R}_0 = 17$, $m = 0.01$ **Figure 6:** An approximate stochastic simulation using the adaptive tau-leaping method.

Figure 7: 3D plots of the probability of coherence at \mathcal{R}_0 values between 2 and 30, and m values between 0 and 0.9.



predicted to reduce the likelihood of the "rescue effect" [2], it should be noted that other parameters such as the number of secondary infections, \mathcal{R}_0 , would be affected by any change in m . Consequently, further study on the effect of changing the mixing parameter in a system should be conducted prior to employing this result as a viable option to controlling epidemics.

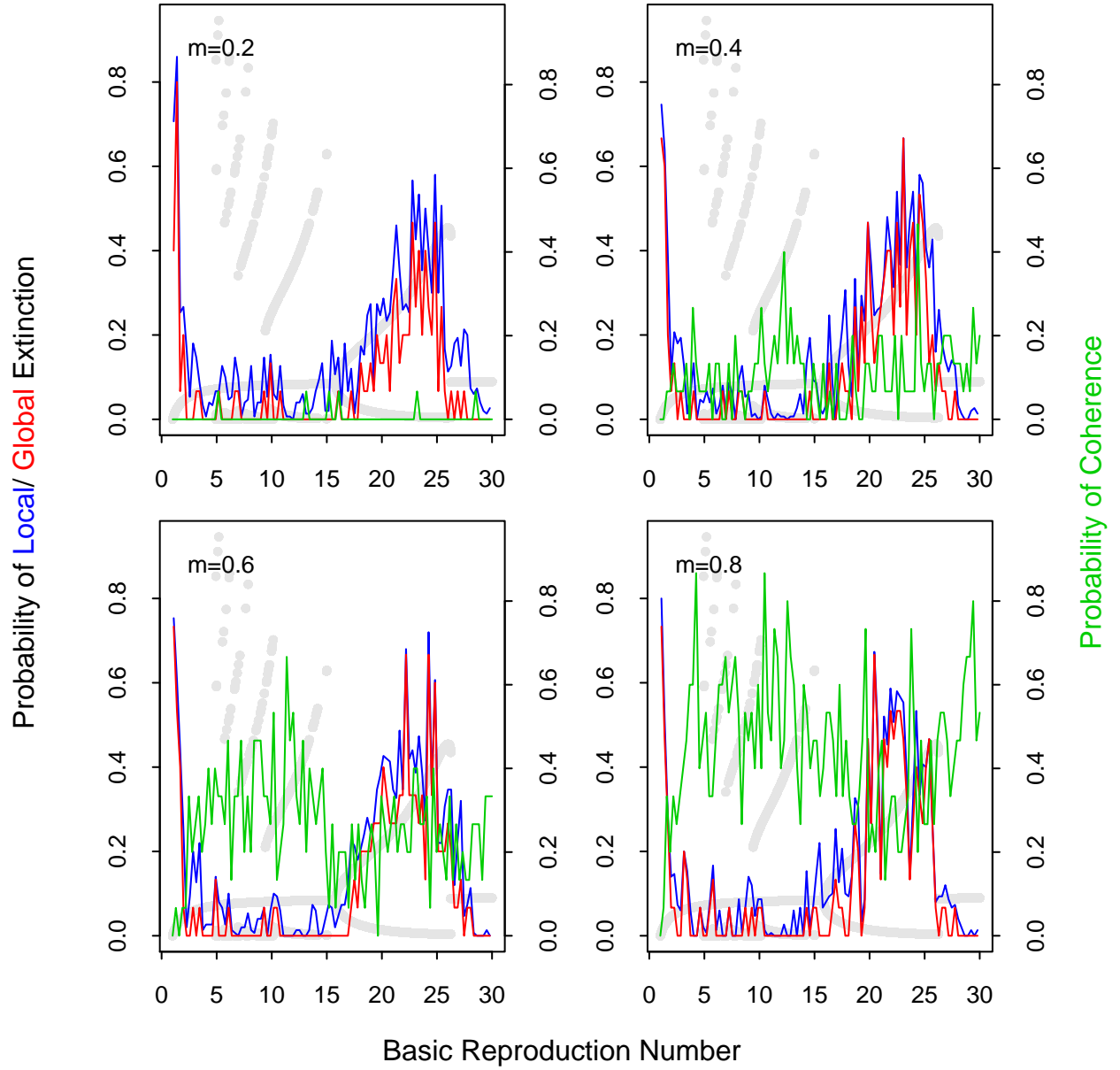
The system under equal coupling and nearest neighbour coupling exhibit similar dynamics, as shown in Fig. 3, with convergence to a coherent solution occurring much slower for the nearest neighbour system. This relationship is expected as already established, coherence increases with the degree of mixing. Since the system under nearest neighbour coupling models less interpatch mixing overall, in comparison with equal coupling, for both models under identical conditions, the one with nearest neighbour coupling should converge slower than the one with equal coupling. Alternate connectivity relations can be investigated to validate that this property has no effect on the overall convergence of the system to coherence, only the time scale in which the result can be predicted to occur.

Through Fig. 7, there appears to be a relation between the basic reproduction number [Note: If possible, change axis name to "Number" en lieu of "Rate" - presentation] and coherence, with the surface appearing to display concavities at certain regions of \mathcal{R}_0 . This relationship is further explored in

Fig. 8 where, for high mixing, coherence is clearly seen to dip in regions corresponding to periods of less complex dynamics, especially in the period of bi-annual cycles between $15 < \mathcal{R}_0 < 25$. But, this pattern of dipping is not seen in the period of annual cycles between $\{5 < \mathcal{R}_0\} \cap \{\mathcal{R}_0 > 27\}$. Therefore, as stated in Earn, Levin, and Rohani, the results indicate that there is only a weak, if any, relation between chaos and population persistence [2] and therefore, that of the parameter \mathcal{R}_0 and coherence.

Instead, more consideration should be directed toward the deviations between local and global extinction in relation to probability of coherence [2, 7]. Deviations are lower for high mixing parameter and dips in global extinction rate in comparison to local extinction rate correspond closely to dips in coherence [Note: May be too similar to what is stated in Earn2000 - pg.2 col.3 p.2 l.1]. In context, this result implies that, for low coherence, the probability of global extinction is also relatively low. This is due to the fact that, while the probability of local extinction is relatively higher, coherence is low, so mixing from other patches at possibly higher rates of infecteds can lead to a rekindling of the disease in patches where local extinction occurred, that is, the "rescue effect" causing global extinction to stay proportionally low.

Figure 8: The probability of coherence, local extinction, and global extinction at \mathcal{R}_0 values between 2 and 30 for four different m values. Below each plot is the bifurcation diagram of the single patch model.



6 CONCLUSION

BIBLIOGRAPHY

- [1] C. Connell McCluskey and David J D Earn. Attractivity of coherent manifolds in metapopulation models. *Journal of Mathematical Biology*, 62(4):509–541, 2011.
- [2] David Earn, Simon Levin, and Pejman Rohani. Coherence and Conservation. *Science*, 290(5495):1360–1364, 2000.
- [3] G. P. Samanta. Analysis of a delayed epidemic model with pulse vaccination. *Chaos, Solitons and Fractals*, 66:74–85, 2014.
- [4] Alun L. Lloyd and Robert May. Spatial Heterogeneity in Epidemic Models. *J. theor. Biol*, 179:1–11, 1996.
- [5] B T Grenfell, O N Bjørnstad, and J Kappey. Travelling waves and spatial hierarchies in measles epidemics. *Nature*, 414(6865):716–23, 2001.
- [6] Jackson Burton, Lora Billings, Derek A T Cummings, and Ira B. Schwartz. Disease persistence in epidemiological models: The interplay between vaccination and migration. *Mathematical Biosciences*, 239(1):91–96, 2012.
- [7] M. Heino, V. Kaitala, E. Ranta, and J. Lindström. Synchronous dynamics and rates of extinction in spatially structured populations. *Proceedings of the Royal Society of London B: Biological Sciences*, 264(1381):481–486, 1997.